Pore structure of aluminas derived from the alkyl derivatives of boehmite

Sung-Wook Kim, Shinji Iwamoto, Masashi Inoue*

Department of Energy and Hydrocarbon Chemistry, Graduate School of Engineering,

Kyoto University, Katsura, Kyoto 615-8510, Japan

Corresponding author. Tel.: +81-75-383-2478; fax: 81-75-383-2479.

E-mail address: inoue@scl.kyoto-u.ac.jp (M. Inoue)

Abstract

The alkyl derivatives of boehmite (alkoxyalumoxanes; $AlO(OH)_{1-x}(OR)_x$) were synthesized by the reaction of aluminum triisopropoxide in straight-chain primary alcohols at 300 °C for 2 h in an autoclave. In the present work, pore structures of aluminas obtained by calcination of the alkyl derivative of boehmite were examined. The alumina obtained from the ethyl derivative of boehmite had a broad pore-size distribution, while the pore-size of the alumina obtained from the dodecyl derivative of boehmite distributed in a narrow range in the mesopore region. The mode pore diameter of the latter alumina increased with the increase in calcination temperature (as-syn., 39 Å; 600 °C, 54 Å; 800 °C, 58 Å; 1000 °C, 68 Å), but narrow pore-size distribution was maintained even after calcination at high temperatures.

Keywords: Alumina; Pore structure; Solvothermal reaction

1. Introduction

For the supports of industrial catalysts, alumina is most widely used because it is inexpensive and reasonably stable, and is provided with a wide range of surface areas and porosities suitable for a variety of catalyst application [1]. Preparation of alumina (or alumina-based) supports with the controlled pore structure is still active area: Thus, many papers have been reported [2–8].

Boehmite is one of the modifications of aluminum oxide hydroxide, AlOOH, and it can be easily prepared by hydrothermal treatment of aluminum hydroxide [9]. Microcrystalline boehmite is called “pseudoboehmite” and is used as a precursor of aluminas. Although boehmite has a layer structure, intercalation of guest molecules into the boehmite layers has never been reported, presumably because of strong hydrogen bonding between the layers. On the other hand, during the course of our long-term study on controlling the pore texture of alumina for use as catalyst supports, we found that the thermal treatment (glycothermal and alcohothermal treatments) of aluminum triisopropoxide (AIP) in organic solvents (glycols and alcohols) yielded novel derivatives of boehmite, in which the alkyl (or hydroxyalkyl) groups were incorporated into the boehmite layers through the covalent bondings [10–13].

In the present work, the pore structures of aluminas derived from the alkyl

derivatives of boehmite were examined.

2. Experimental

2.1. Synthesis of the alkyl derivatives of boehmite

In a Pyrex test tube serving as an autoclave liner, 130 ml of a straight-chain primary alcohol (ethanol, EtOH; 1-butanol, BuOH; 1-pentanol, PeOH; 1-hexanol, HeOH; 1-octanol, OcOH; 1-decanol, DeOH; 1-dodecanol, DDOH) and 12.5 g of aluminum triisopropoxide (AIP) were placed, and the test tube was then placed in a 300 ml autoclave. In the gap between the autoclave wall and the test tube was placed an additional 30 ml of the alcohol. The autoclave was thoroughly purged with nitrogen, heated to 300 ºC at a rate of 2.3 ºC /min, and held at that temperature for 2 h. After the mixture was cooled to room temperature, the resulting precipitate was washed by repeated cycles of agitation with methanol, centrifuging, and decantation, and then air-dried. The obtained product was calcined at the various temperatures by heating at a rate of 10 ºC /min and holding at that temperature for 30 min in a furnace in static air.

These products will be designated by “A” followed by the abbreviation for the medium used in the alcohothermal treatment and calcination temperature in degree

Celsius in parentheses. The original samples will be specified by a term, “as-syn”, in parentheses.

2.2. Characterization.

Powder X-ray diffraction (XRD) was measured on a Shimadzu XD-D1 diffractometer using CuKα radiation and a carbon monochromator. The nitrogen adsorption isotherms were measured at liquid-nitrogen temperature by using a volumetric gas-sorption system, Quantachrome Autosorb-1. The alumina samples were previously outgassed at 300 ºC for 30 min. Surface areas were calculated by applying the BET method to the adsorption data, taking the average area occupied by a nitrogen molecule as 0.162 nm^2. Pore size distributions were calculated from the desorption branch of the nitrogen adsorption isotherm by the BJH method. Infrared spectra were obtained on JASCO FT/IR-470 plus spectrometer using the usual KBr-pellet technique with 128 integration times. Simultaneous thermogravimetric (TG) and differential thermal analyses (DTA) were performed on a Shimadzu DTG-50 analyzer: a weighed amount (ca. 20 mg) of the sample was placed in the analyzer, and then heated at the rate of 10 ºC/min. Morphologies of the products were observed with a scanning electron microscope (SEM), Hitachi S-2500X.

3. Results and discussion

3.1. Alkyl derivatives of boehmite obtained by solvothermal method.

The XRD patterns of the products are shown in Fig. 1. For comparison, the XRD pattern of pseudoboehmite is also given in the figure. The XRD peaks at the high angle side (2θ = 50º and 65º) correspond to the lattice parameters, *a* and *c*, of pseudoboehmite (200 and 002 planes), and the obtained products could be indexed on the basis of the boehmite structure [12,13]. The 020 plane of products shifted toward the lower-angle side with the increase in the carbon number of the alcohol used as the solvent (Fig. 1), suggesting that the alkyl groups derived from the solvent alcohol are incorporated between the boehmite layers. In the XRD patterns of ADeOH(as-syn) and ADDOH(as-syn), the peak due to 020 plane was not clearly shown. The alkyl chains of the decyl and dodecyl groups are so long, that the diffraction peaks for the 020 plane (basal plane) of ADeOH and ADDOH appeared at $2\theta < 3^{o}$. However, they exhibited the 040 and 060 diffraction peaks (these peaks are 2nd and 3rd order diffraction peaks of the basal plane), and therefore the position of the 020 diffraction peak can be calculated precisely from these peaks, which clearly shows the low-angle shift of the 020 diffraction peak. To clarify these points, the 040 and 060 diffraction peaks are indexed in Fig. 1. Linear increase of basal spacing with the increase of carbon number

of solvents was observed (Supplementary materials, Fig. 1S), which is an incontestable evidence for the incorporation of the alkyl groups derived from the solvent alcohols.

In the IR spectra of the products shown in Fig. 2, bands characteristic of the boehmite layers are seen at around 615 and 480 cm^{-1} [14–16], suggesting that the products had the layer structure of boehmite. Bands due to the incorporated organic moieties were also noted at 3000–2850 cm^{-1} (ν_{CH}).

Figure 3 shows the results for thermal analyses of the products. A large weight decrease is seen around 100 and 400 ^{o}C for all of the samples. In the DTA profiles of the products, one endothermic and two exothermic processes took place at around 100, 300 and 400 ^{o}C, respectively. The first process is attributed to desorption of physisorbed water/methanol and the second and third processes are caused by combustion of the alkyl moieties incorporated between the boehmite layers. Collapse of the boehmite layers yielding amorphous alumina seems to take place simultaneously with the last process because of large exothermic effects. Because the molecular weight of ethanol is small as compared to the other alcohols used in this study, the intensity of the exothermic peak as well as the total weight decrease is the smallest among the samples. The exothermic peak shifted slightly toward lower temperature when a long chain alcohol was used (AEtOH(as-syn); 425 ºC, AHeOH(as-syn); 407 ºC

ADDOH(as-syn); 373 ºC). This result may be attributed to the fact that the octane number of an alcohol having a shorter alkyl chain is higher than that of alcohol having a longer alkyl chain [17]. The results of thermal analyses of the products obtained by the reaction of AIP in primary alcohols are summarized in Table 1. All these results are consistent with the fact that the alkyl moieties are incorporated between the boehmite layers.

3.2. Morphological aspects.

The scanning electron micrographs of the products are shown in Fig. 4. Particles of the product obtained in ethanol (AEtOH(as-syn)) had a rod shape. On the other hand, particles of APeOH(as-syn) had irregular shapes but rod shape particles were also seen together with the irregularly-shaped particles. AHeOH(as-syn) and ADDOH(as-syn) were composed of large aggregate particles having irregular shapes.

3.3. Calcined products.

Phase transformation of the alkyl derivatives of boehmite was investigated and Fig. 5 shows the transformation of AHeOH as the representative results. AHeOH maintained the boehmite structure at 300 ^{o}C and converted to amorphous alumina at

400 ^{o}C (Fig. 5). The γ-phase appeared by calcination in air at 800 ^{o}C for 30 min. The sample calcined at 1000 ^{o}C was composed of θ- and α-phases. The single-phase of α-phase was obtained by calcination at 1200 ^{o}C.

All of the other alkyl derivatives of boehmite were converted into γ-alumina through an amorphous phase by calcination at 1000 ^{o}C in air, and the XRD patterns were essentially identical irrespective of the solvents used.

Nitrogen adsorption isotherms, and pore size distribution curves of some the products are shown in Figs. 6–8 and *t*-plots of all the products examined in this paper are given in Fig. 9.

Although the aluminas derived from the ethyl derivative of boehmite exhibited rather complex N_2-adsorption isotherms (Fig. 6a), the *t*-plots (Fig. 9a) derived from the isotherms can be divided into 5 segments. At low *t* (statistical thickness; 0−3 Å) region (corresponding to low partial pressure of nitrogen), the plot seems to have a rather steep slope going through the origin, although only a few data points are available. In the second segment (3−7 Å), the slope decreased. The slope increased in the third segment (7−12 Å) and decreased again in the forth segment (12−18 Å) with final increase at higher *t* region (>18 Å; fifth segment). The decrease of the slope from the first to second segment is a typical phenomenon for microporous materials and is

explained by micropore filling. It was reported that calcination of well-crystallized boehmite gives alumina having micropores with a slit-shape [18,19]. The crystallite sizes of the present products were relatively large, and much larger than pseudoboehmite usually obtained in aqueous systems. Therefore, the boehmite layer structure seems to give the slit-shaped micropores on calcination. Hysteresis loop observed in the isotherms (Fig. 6a) supports the presence of slit-shaped pores in the AEtOH(600).

The increase in the slope at the middle partial pressure region (third segment) can be explained by capillary condensation of adsorbate molecules into mesopores. Gradual decrease in the slope in the third and forth segments suggests that the pore size distributed widely, which is verified by the pore-size distribution curve calculated by the BJH method (Fig. 6b). These pores seem to be formed in the rod-shaped pseudomorphous particles because of the difference between the true densities of γ-alumina and the ethyl derivative of boehmite. The large slope in the fifth segment indicates the presence of macropores, which can be also recognized from the pore-size distribution curve shown in Fig. 6b. Since the pore size is in the order of the size of rod-shaped particles, these pores are formed between pseudomorphous rod-shaped particles.

Microporous structure of AEtOH(as-syn) is due to the elimination of a part of the alkyl groups during the drying stage prior to the N_2-adsorption measurement. Calcination of the product developed micro- and meso-pores because of elimination of ethyl groups and collapse of the boehmite layer structure. Significant increase in mesopore volume is apparent. Further increase in the calcination temperature caused a significant decrease in micropore volume while mesopore volume was slightly decreased. This result suggests that the primary particles of alumina separated by micropores are easily sintered by heat treatment. On the other hand, macropores formed between the rod-shaped particles was not affected by calcination. This can be recognized by essentially identical slopes in the fifth segment and also by the pore-size distribution curves.

The aluminas derived from ABuOH showed *t*-plots (Fig. 9b) different from those obtained from AEtOH. The decrease of the slope from the first to second segments was not seen, indicating that the micropores were not present in the samples. The increase in the slope from the second to third segment was significant and third and forth segments are clearly distinguished, indicating that the pore size distributed in a narrow range, which is verified by the pore-size distribution curve (Fig. 7b). Macropores were not recognized. Hysteresis loop of these products suggests that tubular pores with

narrow constriction were formed (Fig. 7a).

Nitrogen adsorption isotherms of AOcOH exhibited a similar tendency with ABuOH. However, an abrupt increase in the slope at high *t* region (fifth segment) was observed in AOcOH (Fig. 9e), indicating that macropores were present in these samples.

As for APeOH(600) and AHeOH(600), micropores were not recognized and the first and second segments are merged into one line going through the origin (Figs. 9c and 9d). This result can be explained by the boehmite layers separated by long alkyl groups. The forth and fifth segments are also merged. Usually the slope at high *t* region (forth segment) corresponds to the outer surface area after mesopores are filled by adsorbate molecules by capillary condensation. However, this is not the case because the slope at this region is much lager than the slope at low *t* region (the first segment; corresponding to the total surface area). Therefore, pores are formed between the irregularly-shaped particles (Fig. 4c) and the size of these pores distributes widely from meso- to macro- pore region.

The most significant difference between the *t* plots of AHeOH(1000) and ADDOH(1000)A is found in the slope at higher *t* region (Fig. 9f). Since the slope for ADDOH(1000) is smaller than the slope at low *t* region, the former corresponds to the outer surface area of the irregularly-shaped particles shown in Fig. 5d. The particles

size was so large that the space between these particles is not recognized as pores by the nitrogen adsorption method.

The pore sizes of the aluminas derived from ADDOH(as-syn) can be assessed either by closure points of the hysteresis in the isotherms (Fig. 8a), by the regions of the third segments in the *t*-plots (Fig. 9f) or by the pore-size distribution curves (Fig. 8b). All the data suggest that the pore size increased with the increase in the calcination temperature. However, the increase in the pore size by the increase in the calcination temperature is much smaller than that for the ordinary aluminas derived from pseudoboehmite and crystalline aluminum hydroxides [20]. This indicates robustness of the pore structure of the alumina derived from the dodecyl derivative of boehmite, which is attributed to the well-developed layer structure of the precursor due to the strong interaction between the alkyl groups. Table 2 summarized the results for the physical properties of the products.

4. Conclusions

The alumina derived from the ethyl derivative of boehmite had a broad pore-size distribution, while the pore-size of the aluminas obtained from the alkyl derivatives of boehmite with long alkyl chains distributed in a narrow range in the mesopore region.

The mode pore diameter of the latter aluminas increased with an increase in calcination temperature (as-syn., 39 Å; 600 °C, 54 Å; 800 °C, 58 Å; 1000 °C, 68 Å; for ADDOH), but narrow pore-size distribution was maintained even after calcination at high temperatures. These results indicate that van der Waals interaction between the alkyl chains facilitated the formation of the boehmite layers having a fewer number of defects, and that the collapse of the well-developed boehmite layers gave aluminas with narrow pore-size distributions.

References

[1] D.L. Trimm, A. Stanislaus, Appl. Catal. 21 (1986) 215.

[2] A.C. Pierre, E. Elaloui, G.M. Pajonk, Langmuir 14 (1998) 66.

[3] F. Vaudry, S. Khodabandeh, M.E. Davis, Chem. Mater. 8 (1996) 1451.

[4] S.A. Bagshaw, T.J. Pinnavaia, Angew. Chem. Int. Ed. Engl. 35 (1996) 1102.

[5] W. Zhang, T.J. Pinnavaia, Chem. Commun. (1998) 1185.

[6] S. Valange, J.-L. Guth, F. Kolenda, S. Lacombe, Z. Gabelica, Microporous Mesoporous Mater. 35-36 (2000) 597.

[7] X. Zhang, F. Zhang, K.-Y. Chan, Mater. Lett. 58 (2004) 2872.

[8] W.-C. Li, A.-H. Lu, W. Schmidt, F. Schüth, Chem. Eur. J. 11 (2005) 1658.

[9] A. Ionescu, A. Allouche, J.-P. Aycard, M. Rajzmann, F. Hutschka, J. Phys. Chem. B

106 (2002) 9359.

[10] M. Inoue, H. Kominami, T. Inui, J. Am. Ceram. Soc. 73 (1990) 1100.

[11] M. Inoue, M. Kimura, T. Inui, Chem. Mater. 12 (2000) 55.

[12] M. Inoue, Y. Kondo, T. Inui, Inorg. Chem. 27 (1988) 215.

[13] M. Inoue, H. Tanino, Y. Kondo, T. Inui, Clays Clay Miner. 39 (1991) 151.

[14] J.J. Fripiat, H. Bosmans, P.G. Rouxhet, J. Phys. Chem. 71 (1967) 1097.

[15] M.C. Stegmann, D. Vivien, C. Mazieres, Spectrichim. Acta, Part A 29A (1973) 1653.

[16] A.B. Kiss, G. Keresztury, L. Farkas, Spectrochim. Acta. Part A 36A (1980) 653.

[17] Y. Yacoub, R. Bata, M. Gautam, Proc. Instn. Mech. Engrs. Part A 212 (1998) 363.

[18] J.H. de Boer, B.C. Lippens, J. Catal. 3 (1964) 38.

[19] B.C. Lippens, J.H. de Boer, J. Catal. 4 (1965) 319.

[20] T. Inui, T. Miyake, Y. Takegami, J. Jpn. Petrol. Inst. 25 (1983) 242.

Figure captions

Fig. 1. XRD patterns of pseudoboehmite (h) and the products (a–g) obtained by reaction of AIP in alcohols: a, AEtOH(as-syn); b, ABuOH(as-syn); c, APeOH(as-syn); d, AHeOH(as-syn); e, AOcOH(as-syn); f, ADeOH(as-syn); g, ADDOH(as-syn).

Fig. 2. IR spectra of the products obtained by the reaction of AIP in alcohols: a, AEtOH(as-syn); b, AHeOH(as-syn); c, ADDOH(as-syn).

Fig. 3. Thermal analyses of the products obtained by the reaction of AIP in the alcohols specified in the figure, in a 40 ml/min flow of dried air at the heating rate of 10 ºC /min: a, TG; b, DTA.

Fig. 4. Scanning electron micrographs of the products: a, AEtOH(as-syn); b, APeOH(as-syn); c, AHeOH(as-syn); d, ADDOH(as-syn).

Fig. 5. XRD patterns of aluminas obtained by calcinaton of the hexyl derivative of boehmite at various temperature in air: a, 300 ºC; b, 400 ºC; c, 500 ºC; d, 600 ºC; e, 800 ºC; f, 1000 ºC; g, 1100 ºC; h, 1200 ºC.

Fig. 6. Nitrogen adsorption isotherms (a) and *t*-plots (b) of the aluminas obtained by calcinaton of the ethyl derivative of boehmite at various temperatures.

Fig. 7. Nitrogen adsorption isotherms (a) and *t*-plots (b) of the aluminas obtained by calcinaton of the butly derivative of boehmite at various temperatures.

Fig. 8. Nitrogen adsorption isotherms (a) and *t*-plots (b) of the aluminas obtained by calcinaton of the dodecyl derivative of boehmite at various temperatures.

Fig. 9. *t*-Plots of the aluminas obtained by calcinaton of the alkyl derivatives of boehmite at various temperatures: (a) ethyl derivative boehmite; (b) butyl derivative boehmite; (c) pentyl derivative boehmite; (d) hexyl derivative boehmite; (e) octyl derivative boehmite; (f) dodecyl derivative boehmite.

Table 1

Summary of thermal analysis of the alkyl derivatives of boehmite obtained by solvothermal method.

Sample	Weight ratio (BD^a/Al_2O_3)	Ignition temperature (^oC)	Molecular fomular[b]
AEtOH	1.25	425	$AlO(OH)_{0.86}(OEt)_{0.14}$
ABuOH	1.25	402	$AlO(OH)_{0.89}(OBu)_{0.11}$
APeOH	1.51	417	$AlO(OH)_{0.76}(OPe)_{0.24}$
AHeOH	1.36	407	$AlO(OH)_{0.89}(OHe)_{0.11}$
AOcOH	1.51	408	$AlO(OH)_{0.85}(OOc)_{0.15}$
ADeOH	1.41	400	$AlO(OH)_{0.91}(ODe)_{0.09}$
ADDOH	1.66	373	$AlO(OH)_{0.85}(ODD)_{0.15}$

a: Alkyl derivatives of boehmite.

b: Empirical formulas, $AlO(OH)_{1-x}(OR)_x$ were calculated from ignition losses determined by TG analysis for the products; Et, CH_3CH_2-; Bu, $CH_3(CH_2)_3$-; Pe, $CH_3(CH_2)_4$-; He, $CH_3(CH_2)_5$-; Oc, $CH_3(CH_2)_7$-; De, $CH_3(CH_2)_9$-; DD, $CH_3(CH_2)_{11}$-

Table 2

Physical properties of the alumina obtained by calcination of alkyl derivatives of boehmite at various temperatures.

Sample	Calcination Temp. (^{o}C)	Surface area (m^2/g)	Pore volume (cc/g)	mode pore size (Å)
AEtOH	as syn.	389	0.74	74
	600	346	1.02	68
	800	167	0.64	63
	1000	117	0.64	80
ABuOH	as syn.	543	0.63	37
	400	414	0.73	50
	600	390	0.73	51
	1000	112	0.37	58
APeOH	600	364	1.0	50
	1000	105	0.56	110
AHeOH	as syn.	389	0.47	90
	600	392	0.69	68
	1000	119	0.51	154
AHOcOH	400	530	1.1	37
	600	513	1.27	50
	1000	136	0.65	62
ADeOH	as syn	444	0.71	37
	400	592	1.3	37
	600	469	1.2	42
	1000	157	0.76	62
ADDOH	as syn.	392	0.54	39
	600	338	0.69	54
	800	258	0.59	58
	1000	111	0.32	68

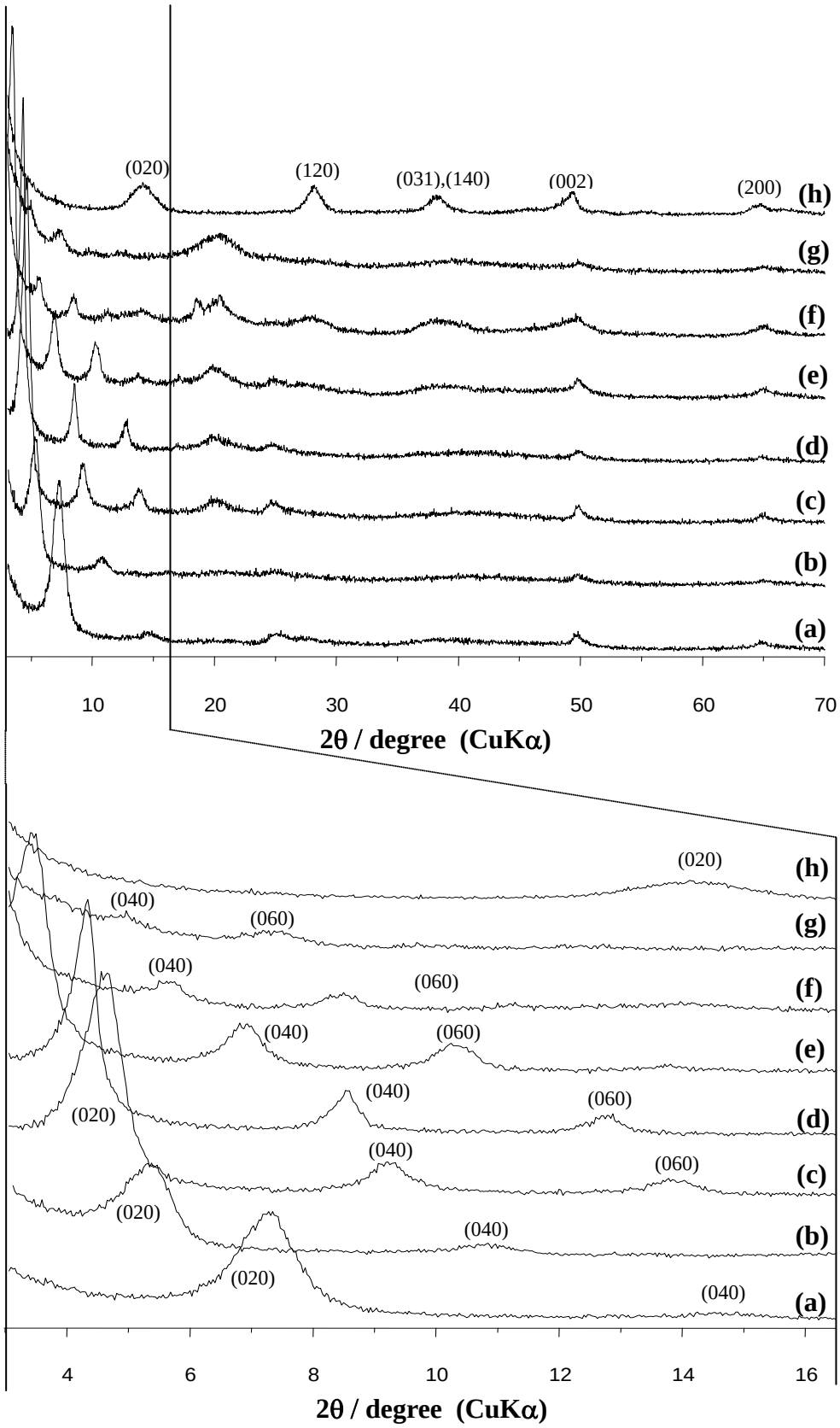

Fig. 1. Kim, et al.

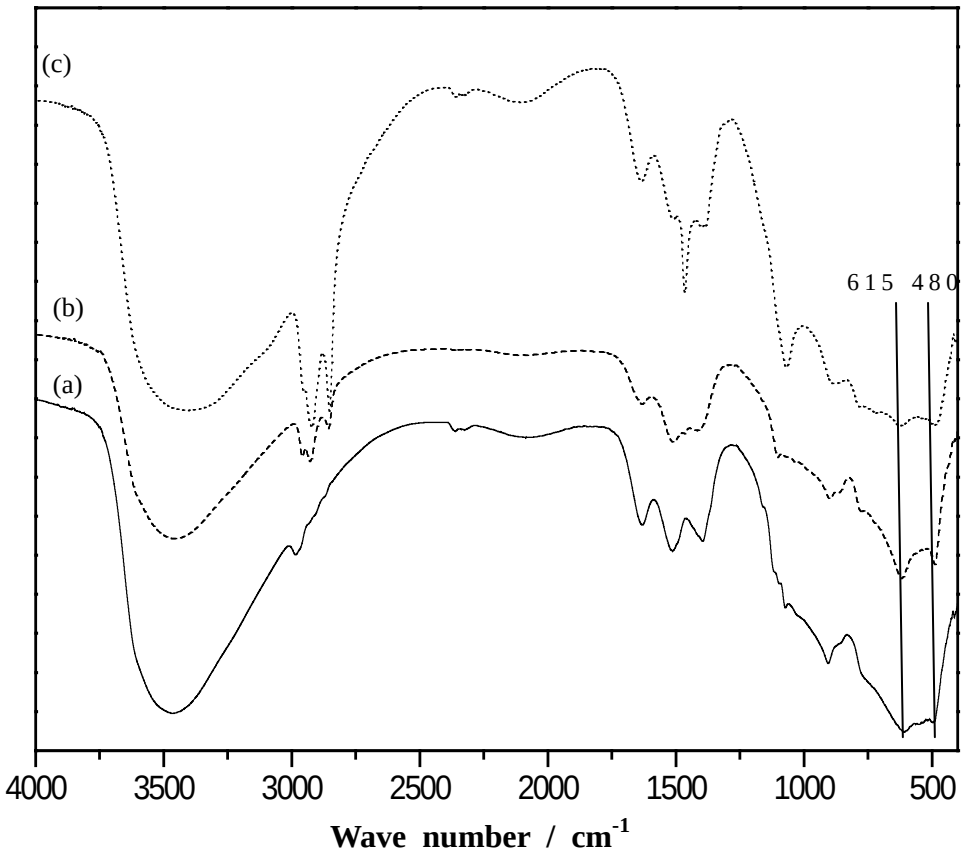

Fig. 2. Kim, et al.

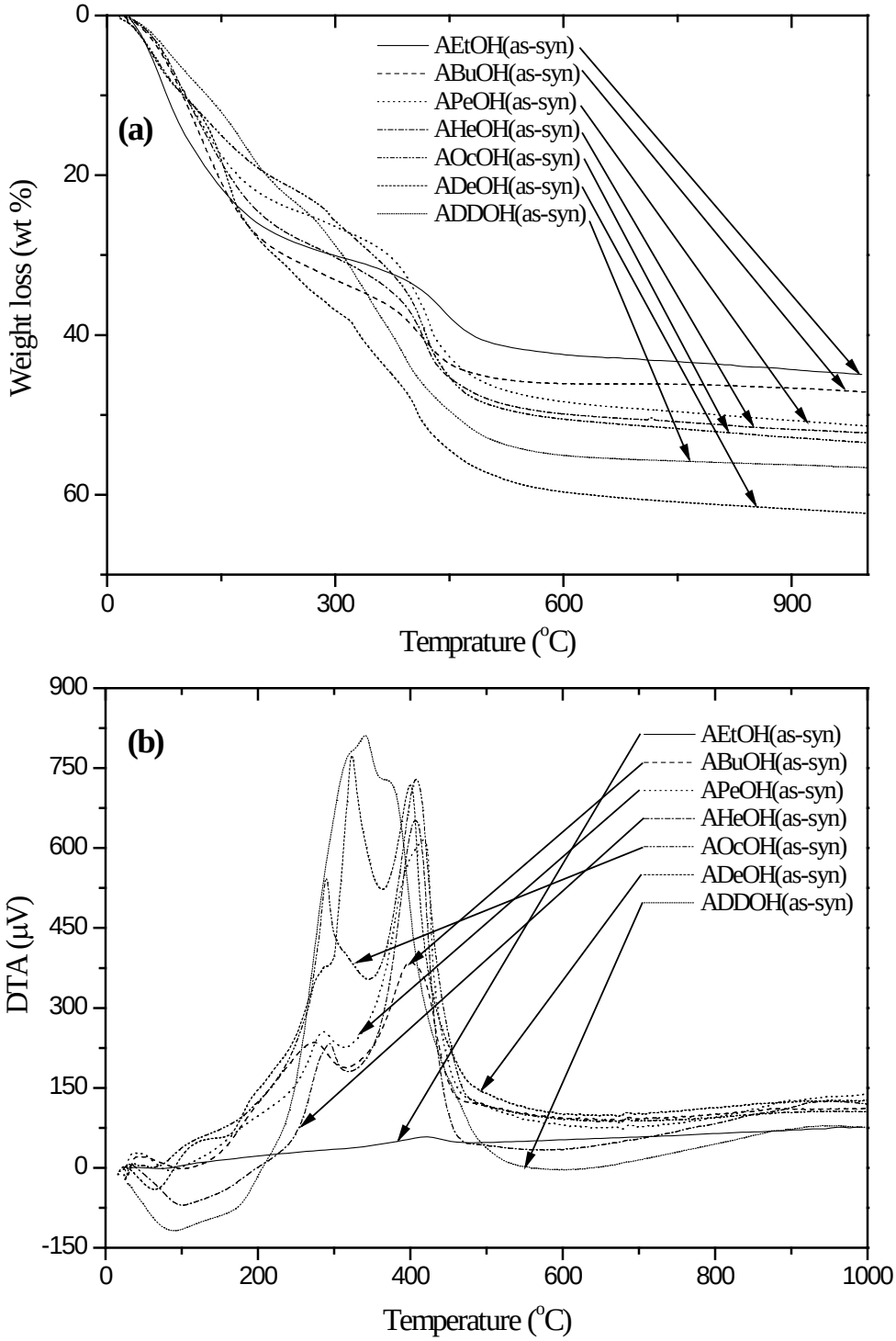

Fig. 3. Kim, et al.

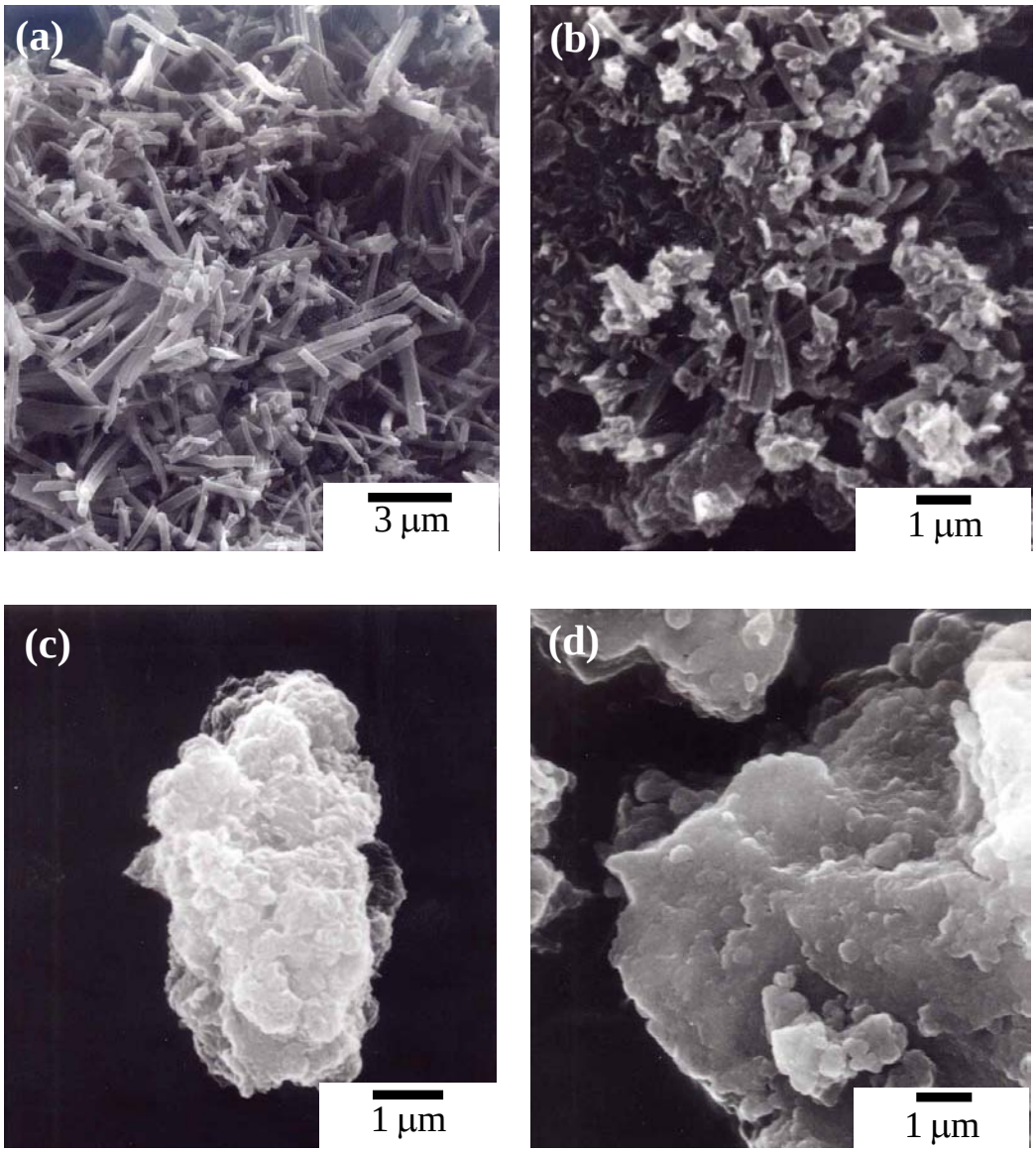

Fig. 4. Kim, et al.

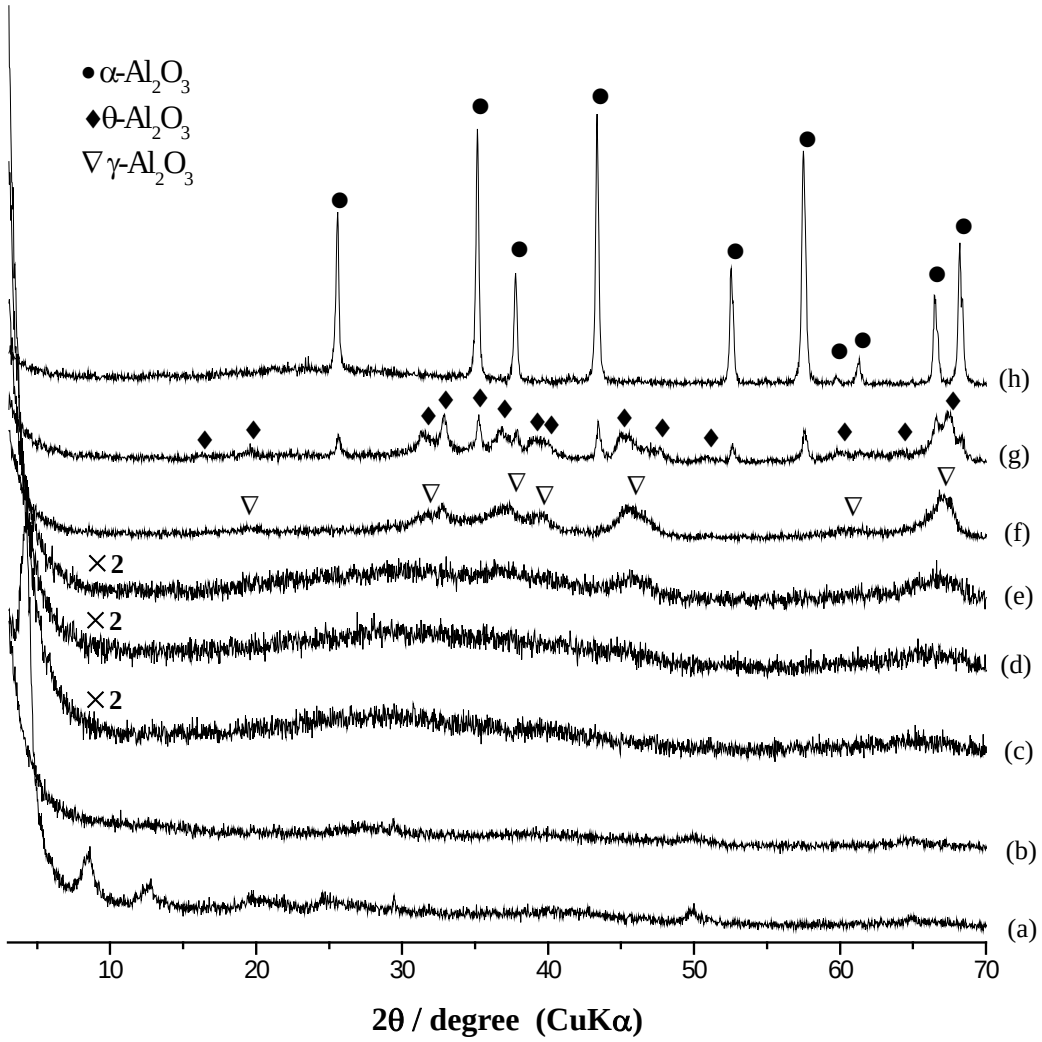

Fig. 5. Kim, et al.

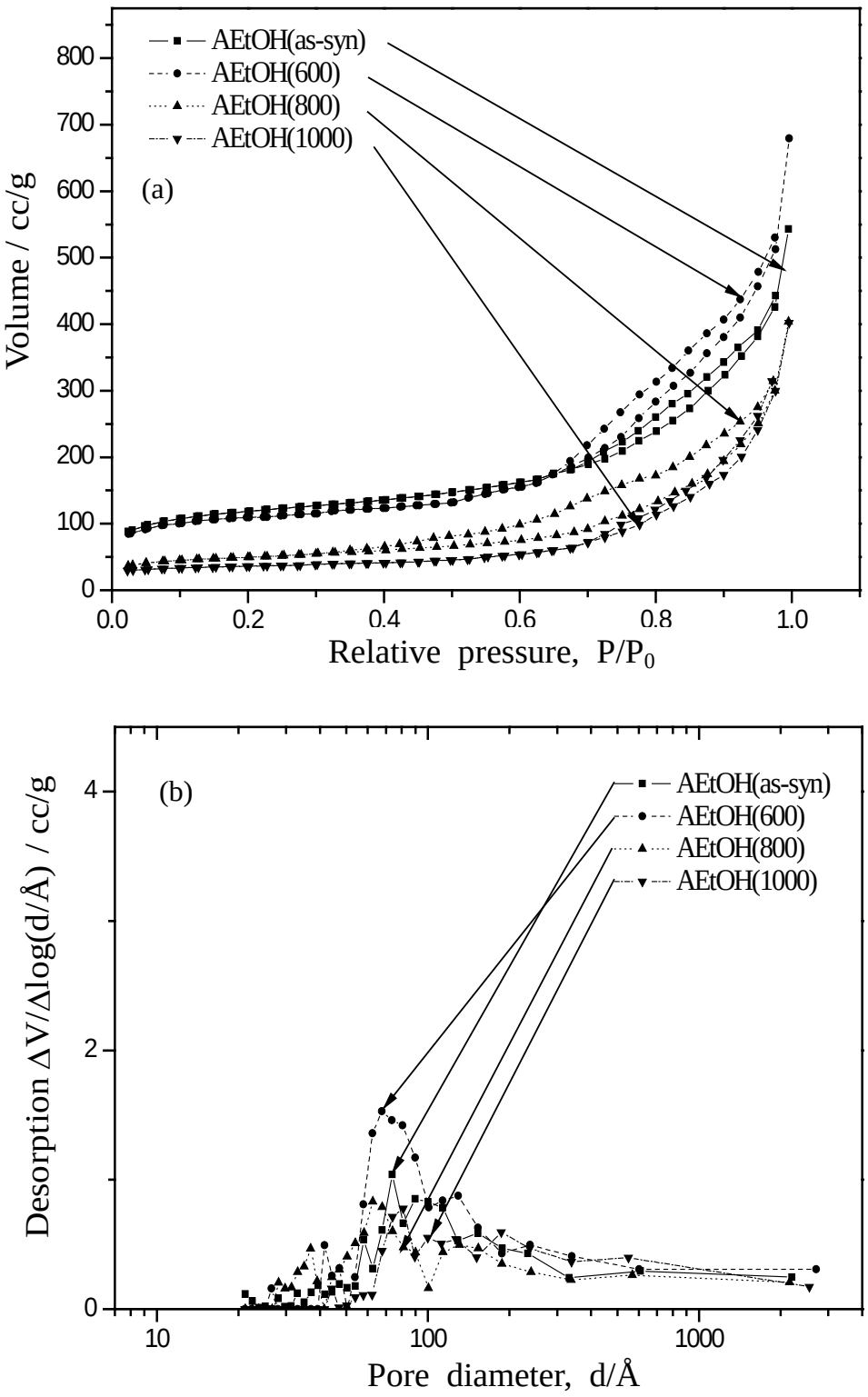

Fig. 6. Kim, et al.

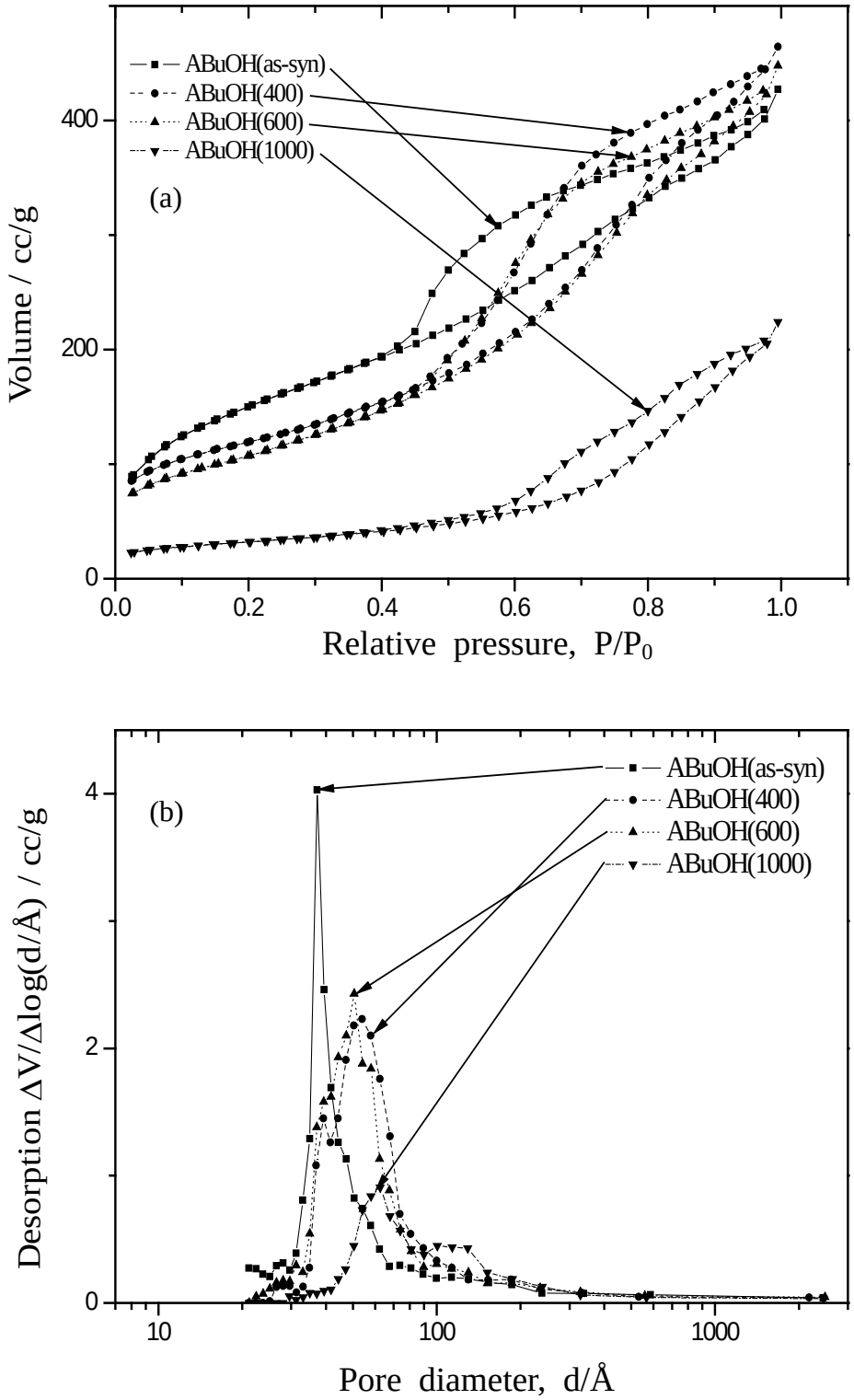

Fig. 7. Kim, et al.

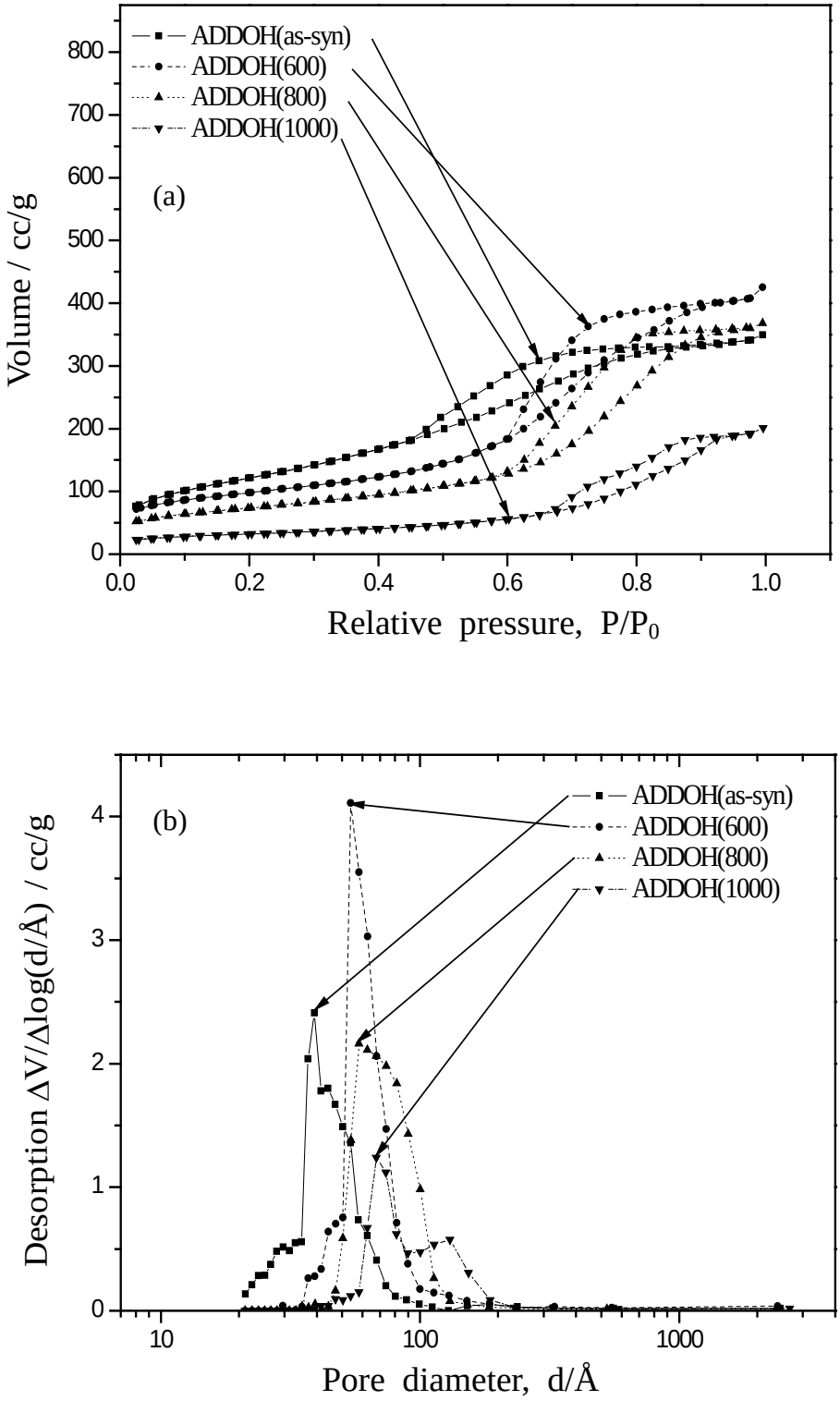

Fig. 8. Kim, et al.

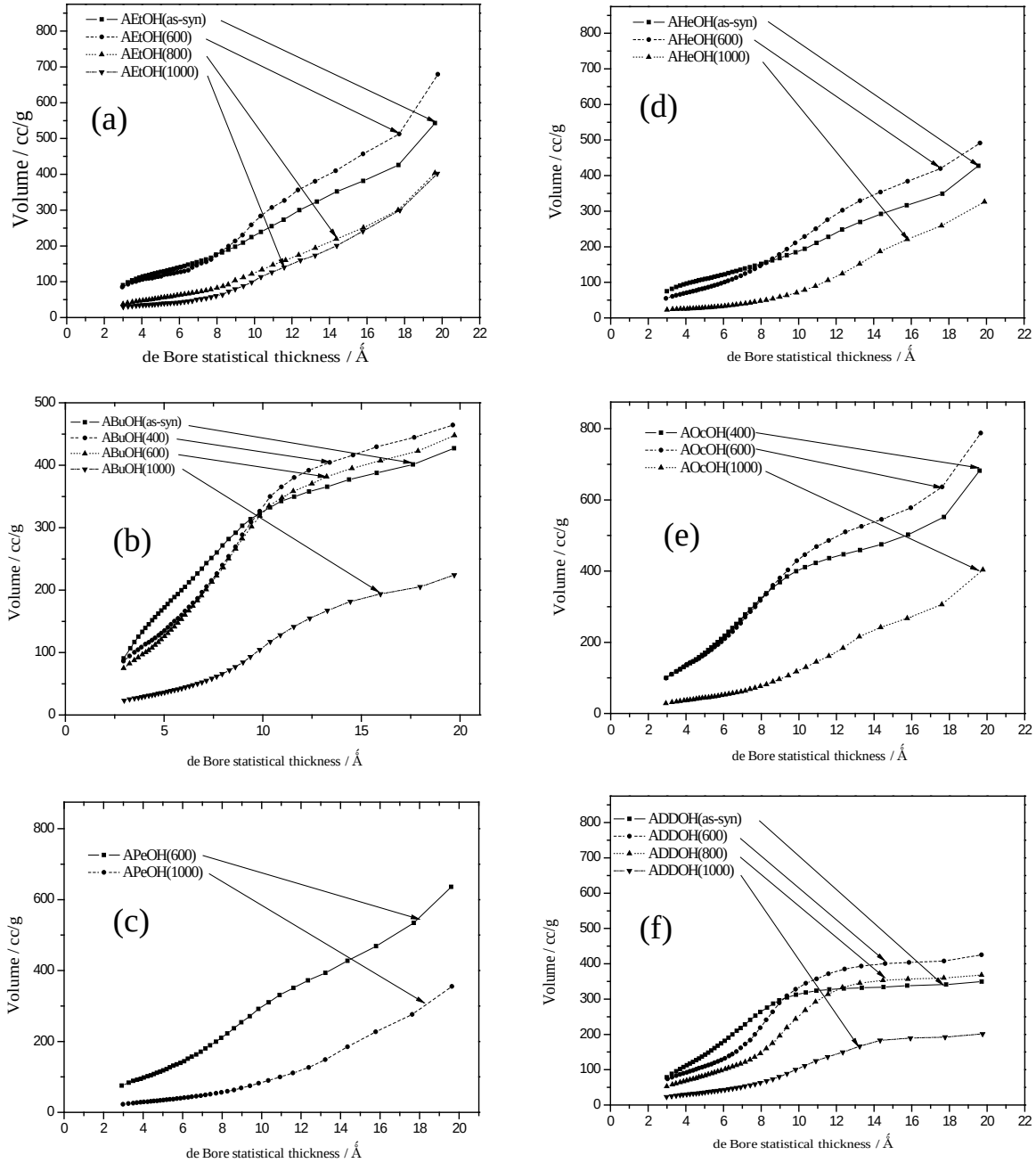

Fig. 9. Kim, et al.